The Astrophysical Journal, 748:95 (10pp), 2012 April 1 doi:10.1088/0004-637X/748/2/95

LABORATORY IR STUDIES AND ASTROPHYSICAL IMPLICATIONS OF C_2H_2-CONTAINING BINARY ICES

C. Knez[1,2], M. H. Moore[3], R. F. Ferrante[4], and R. L. Hudson[3]
[1] Astronomy Department, University of Maryland, College Park, MD 20742, USA; Claudia.Knez@jhuapl.edu
[2] The Johns Hopkins University Applied Physics Laboratory, 11100 Johns Hopkins Rd, Laurel, MD 20723, USA
[3] NASA Goddard Space Flight Center, Astrochemistry Laboratory, Greenbelt, MD 20771, USA
[4] Chemistry Department, U.S. Naval Academy, 572 Holloway Road, Annapolis, MD 21402, USA
Received 2011 May 11; accepted 2012 January 13; published 2012 March 13

ABSTRACT

Studies of molecular hot cores and protostellar environments have shown that the observed abundance of gas-phase acetylene (C_2H_2) cannot be matched by chemical models without the inclusion of C_2H_2 molecules subliming from icy grain mantles. Searches for infrared (IR) spectral features of solid-phase acetylene are under way, but few laboratory reference spectra of C_2H_2 in icy mixtures, which are needed for spectral fits to observational data, have been published. Here, we report a systematic study of the IR spectra of condensed-phase pure acetylene and acetylene in ices dominated by carbon monoxide (CO), carbon dioxide (CO_2), methane (CH_4), and water (H_2O). We present new spectral data for these ices, including band positions and intrinsic band strengths. For each ice mixture and concentration, we also explore the dependence of acetylene's ν_5-band position (743 cm^{-1}, 13.46 μm) and FWHM on temperature. Our results show that the ν_5 feature is much more cleanly resolved in ices dominated by non-polar and low-polarity molecules, specifically CO, CO_2, and CH_4, than in mixtures dominated by H_2O-ice. We compare our laboratory ice spectra with observations of a quiescent region in Serpens.

Key words: infrared: ISM – ISM: lines and bands – ISM: molecules – methods: laboratory

Online-only material: color figure

1. INTRODUCTION

Infrared (IR) absorptions of gas-phase acetylene, C_2H_2, were first identified in interstellar clouds by Lacy et al. (1989), with a reported C_2H_2:CO ratio near 10^{-3} (Lacy et al. 1989; Evans et al. 1991). Gas-phase C_2H_2 also has been detected toward massive young stellar objects (e.g., Lahuis & van Dishoeck 2000) with estimated acetylene column densities near 10^{16} cm^{-2} and C_2H_2 abundances of 0.1–0.5 with respect to $H_2O = 100$. These infrared observations give C_2H_2 column densities that are larger than those predicted by steady-state gas-phase chemical models, suggesting that additional acetylene is contributed by C_2H_2 molecules subliming from icy grains (e.g., Brown et al. 1988; Nguyen et al. 2002; Stäuber et al. 2004, 2005).

Gas-phase acetylene also has been identified in cometary comae and is thought to originate from solid C_2H_2 in the ices of cometary nuclei. This organic molecule has been found in Oort Cloud comets such as Lee, Hale-Bopp, Hyakutake, and Ikeya-Zhang with abundances of 0.1–0.5 relative to $H_2O = 100$ (Mumma et al. 2003, Mumma & Charnley 2011). The chemical composition of ices in such Oort Cloud comets is believed to be representative of the cold interstellar and outer protoplanetary disk regions in which these comets formed.

Cometary comae and interstellar clouds have yielded numerous detections of gas-phase acetylene, but direct evidence for solid-phase C_2H_2, such as in interstellar ices, is also desired. Interstellar ices are found in a variety of environments such as dark clouds and envelopes around protostars. Studies of ices toward background stars, with lines of sight traversing quiescent dense clouds, have been made with the *Spitzer Space Telescope*. Such observations initially focused on the major ice-mantle components, such as H_2O, CO_2, and CO (e.g., Chiar et al. 1994, 1995; Whittet et al. 1996, 1998, and references therein). Detections of these and other molecules are generally favored when either (1) the IR band has a strong intrinsic intensity, a high so-called *A* value, or (2) the target molecule has an IR band of modest intrinsic strength, but lies in a spectral region unobscured by other features, including the broad, intense bands of H_2O-ice. To illustrate the second factor, recent observations toward low-mass protostars with the Infrared Spectrograph on the *Spitzer Space Telescope* (*Spitzer*/IRS) show evidence for CH_4 (Öberg et al. 2008) at 1301 cm^{-1} (7.69 μm). This CH_4-ice feature has only a modest intrinsic strength, but is located in a relatively clear part of the mid-IR spectrum. It is thus possible that other minor species with modest *A* values, including C_2H_2, might also be detected. However, the case for C_2H_2 is complicated by the fact that its strongest features do not lie in a clear part of the mid-IR spectrum, but overlap in position with the broad bands of H_2O-ice. Extraction of any C_2H_2 residual is done by modeling and removing the silicate and water band spectra. Therefore, the position, strength, bandwidth, and profile of C_2H_2 IR features in H_2O and other matrices are needed. These band parameters can be directly compared with astronomical data to understand abundances, temperatures, and the molecular environment of solid C_2H_2.

To date, only one suggested detection of solid-phase C_2H_2 has been made using *Spitzer*/IRS observations of a field star behind the Serpens dense cloud, a region of high star formation activity (Knez et al. 2008). This detection was from the *Spitzer* c2d program and the specific sight line is designated 2MASS 18285266 + 0028242. For convenience, it will be referred to simply as "the Serpens source" in this paper.

Here, we wish to compare recent laboratory results on solid C_2H_2 and C_2H_2-containing two-component ices with the optical depth spectrum of the same Serpens-source spectrum. From laboratory IR studies we know that when C_2H_2 gas is condensed slowly below about 45 K, it forms an amorphous solid. Crystallization takes place on warming this ice to about 50 K. In low-pressure vacuum environments, solid C_2H_2 rapidly sublimes near 85 K. In both phases, frozen C_2H_2 possesses two moderately strong IR-active fundamental vibrations, ν_3 near 3240 cm^{-1} (3.086 μm) and ν_5 near 743 cm^{-1} (13.46 μm),

along with several weak overtone and combination bands. The ν_3 C–H stretching mode is the strongest IR band of C_2H_2 followed by the ν_5 C–H bending vibration. Each band overlaps in position with a strong feature of H_2O-ice, making it difficult to identify C_2H_2 in observations of H_2O-dominated ices. When interpreting *Spitzer*/IRS spectra (5–20 μm region), it is the strong libration mode of H_2O that explains much of the excess absorption at 12–13 μm. Also, because of blending with the silicate absorption feature, any residuals in this region (e.g., the ν_5 band of C_2H_2) are difficult to extract and interpret. For this reason, laboratory studies can be particularly valuable in suggesting specific acetylene-containing ices that might be identifiable, and the conditions under which they might exist in astronomical environments.

Previous laboratory studies of crystalline C_2H_2 include IR spectra (Bottger & Eggers 1964), infrared intensities (Dows 1966), and optical constants (Khanna et al. 1988), all measured at 63–70 K. Only one study of solid C_2H_2, and C_2H_2 mixed with H_2O and CO ices, below 20 K reported both band positions and widths (Boudin et al. 1998). These same authors calculated *A* values for amorphous mixtures of (a) C_2H_2 and H_2O and (b) C_2H_2 and CO at 10 K by scaling them from published band strengths for crystalline C_2H_2 at 65 K (Dows 1966). A study of the 743 cm^{-1} band of C_2H_2 mixed with CO_2 by Gough & Rowat (1998) showed the metastable nature of a CO_2–C_2H_2 complex. In addition, IR absorption spectra of C_2H_2 dispersed in various inert matrices at 10 K have been reported (Lee et al. 2007; George et al. 2003) and can be used as reference spectra to identify small clusters.

We present here an IR spectroscopic study of C_2H_2 ice and binary ices of C_2H_2 mixed with CO, CO_2, CH_4, and H_2O. The motivation for choosing CO, CO_2, and H_2O matrices was that typically they are not only the three most abundant ices in dark clouds (e.g., Gibb et al. 2004; Knez et al. 2005; Boogert et al. 2011; Chiar et al. 2011), but also in low- and high-mass protostellar envelopes (Öberg et al. 2011). We assume that the line of sight to the Serpens source samples a typical dark cloud region. Methane was chosen as a matrix molecule in order to examine the influence of a hydrocarbon environment on acetylene's IR bands. Ice mixtures with matrix:C_2H_2 ratios of 50:1, 10:1, and 1:1 were studied to determine the position and shape of the 743 cm^{-1} (13.46 μm) bending mode of C_2H_2 as a function of temperature (especially over the 20–50 K range). We measured the intrinsic band strengths of pure C_2H_2 and calculated them for icy mixtures. In Section 4, we use this new data to explore the astrophysical implications of our results and also to compare our laboratory spectra with a *Spitzer* observation of the Serpens source.

2. EXPERIMENTAL METHOD

The focus of this work was the influence of composition, phase, and temperature on the mid-IR bands of C_2H_2 in non-polar and polar ices. Spectra were recorded from 4000 to 500 cm^{-1} (2.5–20 μm), although special attention was given to acetylene in the ν_5 region (743 cm^{-1}, 13.46 μm). In some cases, the ν_3 (3239 cm^{-1}, 3.087 μm) and ν_4 + ν_5 (1371 cm^{-1}, 7.294 μm) bands were studied since they too could provide information useful for interpreting astrophysical spectra.

General features of our experimental setup, ice preparation, and IR spectral measurement techniques have been published (e.g., Hudson & Moore 2004; Moore & Hudson 2003). A schematic diagram of the experimental arrangement specific to this work can be seen in Figure 1. Briefly, gas samples of C_2H_2, either pure or mixed with CO, CO_2, CH_4, or H_2O, were prepared in a vacuum manifold using standard manometric techniques. Commercial gases C_2H_2, CO, CO_2, and CH_4 were all Matheson Research Grade. Acetylene was purified before use by distillation from a liquid nitrogen/methanol slush bath (173 K) to remove acetone used as a stabilizer; the other commercial gases were used without further purification. Water was triply distilled and had a resistivity greater than 10^7 ohm cm. Gas mixtures typically were prepared in ratios such as matrix:C_2H_2 = 50:1, 10:1, and 1:1. These ratios were chosen simply to provide a range of conditions, rather than to represent any specific astrophysical environment. The gas mixtures flowed through a controlled leak valve and were then condensed onto a pre-cooled CsI or KRS-5 substrate inside a stainless steel high-vacuum chamber ($\sim 10^{-7}$ torr). To form an ice, the sample gas was deposited at about 3×10^{-6} mol $minute^{-1}$ for approximately 20 minutes, with a total ice thickness of 2–5 μm as determined by a laser interference fringe counting system.

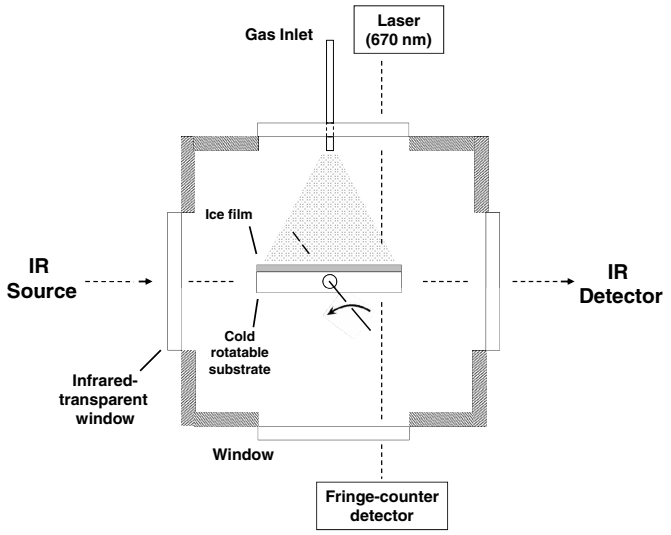

Figure 1. Schematic of experimental setup. The sample chamber has two infrared-transparent windows, and an appropriate substrate onto which the ice film is formed. Infrared spectra are measured when the substrate is rotated 90° from the position shown.

After deposition, samples were rotated to face the beam of the IR spectrometer (Figure 1), and transmission spectra then were recorded from 4000 to 500 cm^{-1} (2.5–20 μm) with a resolution of 4, 2, or 1 cm^{-1}, using 60–100 co-added scans. A typical spectral scan with 2 cm^{-1} resolution required 10 minutes. We used the Mattson Polaris and Perkin-Elmer Spectrum GX Fourier-Transform Infrared spectrometers, each equipped with a room temperature DTGS detector. After the initial spectrum was recorded, samples were warmed to selected temperature points in small increments (usually 3 K) at a rate of 1 K $minute^{-1}$. Spectra were recorded at these points to document any changes in band position and shape. Samples could be maintained at any temperature from 20 to 80 K, with a typical precision of ±1 K.

3. RESULTS

We first present mid-IR spectra of solid C_2H_2 and then spectra of ices made from C_2H_2 mixed with CO, CO_2, CH_4, and H_2O. Along with the full mid-IR spectrum of each ice, we also show details of acetylene's ν_5-band position (840–690 cm^{-1}) and shape as a function of temperature in Section 3.1. In Section 3.2, we give information on the FWHM for acetylene's ν_5 band.

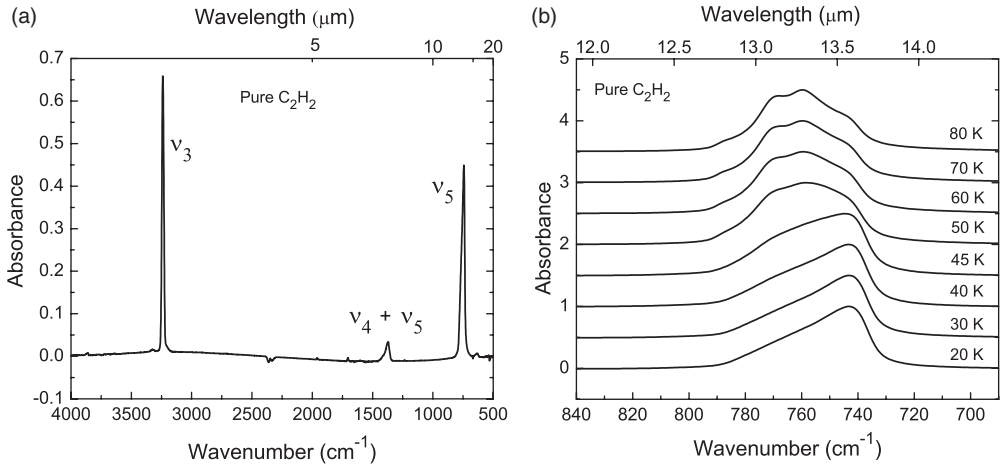

Figure 2. Infrared spectrum of (a) amorphous C_2H_2 at 20 K and (b) an enlargement of the ν_5 region showing the change to a crystalline solid at 50 K. In (b) each spectrum is normalized to 1.

Table 1
Infrared Peak Positions for Amorphous C_2H_2-containing Ices at 20 K[a]

Mode	C_2H_2 (Pure)	CO:C_2H_2 (50:1)	CO_2:C_2H_2 (50:1)	CH_4:C_2H_2 (50:1)	H_2O:C_2H_2 (5:1)
ν_3	3239 (3.087)	3261 (3.067)	3258 (3.069)	3271 (3.057)	...
$\nu_4 + \nu_5$	1371 (7.294)	1372 (7.289)	1384 (7.225)	1338 (7.474)	1421 (7.037)
ν_5	743 (13.46)	765 (13.07)	763 (13.11)	737 (13.57)	757 (13.21)

Note. [a] Positions in cm^{-1} (μm in parentheses).

Table 2
Intrinsic Band Strengths (A) for Amorphous C_2H_2-containing Ices[a]

	This Work $T = 20$ K					Boudin et al. (1998)[b] $T = 10$ K	
Mode	C_2H_2 (Pure)	CO:C_2H_2 (50:1)	CO_2:C_2H_2 (50:1)	CH_4:C_2H_2 (50:1)	H_2O:C_2H_2 (5:1)	CO:C_2H_2 (20:1)	H_2O:C_2H_2 (5:1)
ν_3	16 ± 1.5	53	28	12	...	42	24
$\nu_4 + \nu_5$	2 ± 1	5.4	1.6	1.8	7	7.3	3.6
ν_5	20 ± 3	41	33	20	...	40	...

Notes.
[a] Band strengths in units of 10^{-18} cm molecule^{-1}.
[b] Based on band strengths reported for crystalline C_2H_2 at 65 K by Dows (1966).

3.1. Band Position and Shape

3.1.1. C_2H_2 Ice

The IR spectrum of amorphous C_2H_2 is shown in Figure 2(a) from 4000 to 500 cm^{-1} (2.5–20 μm). Peak positions for the ν_5 and ν_3 fundamentals, and for the $\nu_4 + \nu_5$ combination band, are listed in Table 1. Calculations of intrinsic band strengths, A (cm molecule^{-1}), at 20 K were done using

$$A = \frac{\ln 10 \int \mathrm{Abs}(\tilde{\nu}) d\tilde{\nu}}{N}, \quad (1)$$

where $\int \mathrm{Abs}(\tilde{\nu}) d\tilde{\nu}$ is an IR band's integrated absorbance in cm^{-1}, N is the C_2H_2 column density in molecule cm^{-2}, and the "ln 10" coefficient converts from common to natural logarithms. The column density was calculated from the ice's thickness, which was determined from the number of laser interference fringe maxima recorded as the ice was grown. For each ice, we assumed an index of refraction of 1.4 (Khanna et al. 1988) and a density of 1 g cm^{-3}. Calculated A values are given in Table 2 along with published values.

Figure 2(b) shows changes in the ν_5 band as the ice was warmed. In this figure and similarly in Figures 3–10 where the ν_5 bending mode is plotted, the intensity of the ν_5 feature at each temperature was normalized to 1 to clearly show the band position and shape. Figure 2(b) shows that the band broadened on the long-wavenumber side when the temperature reached 45 K. Additional warming gave complete crystallization near 50 K. This change was corroborated by monitoring the ν_3 band (spectral details not shown). Structure within the crystalline acetylene ν_5 feature may have resulted from the formation of different C_2H_2 aggregates since acetylene has the capacity to self-associate through hydrogen bonding to form dimers and higher associations (Bagdanskis & Bulanin 1972). All C_2H_2 thin film ices sublimed within hours near 85 K in our vacuum system.

3.1.2. CO:C_2H_2 Ice Mixtures

Figure 3(a) shows IR spectra of amorphous CO:C_2H_2 ices compared with spectra of C_2H_2 and CO. For these mixtures, Figure 3(b) shows that dilution with CO caused the acetylene

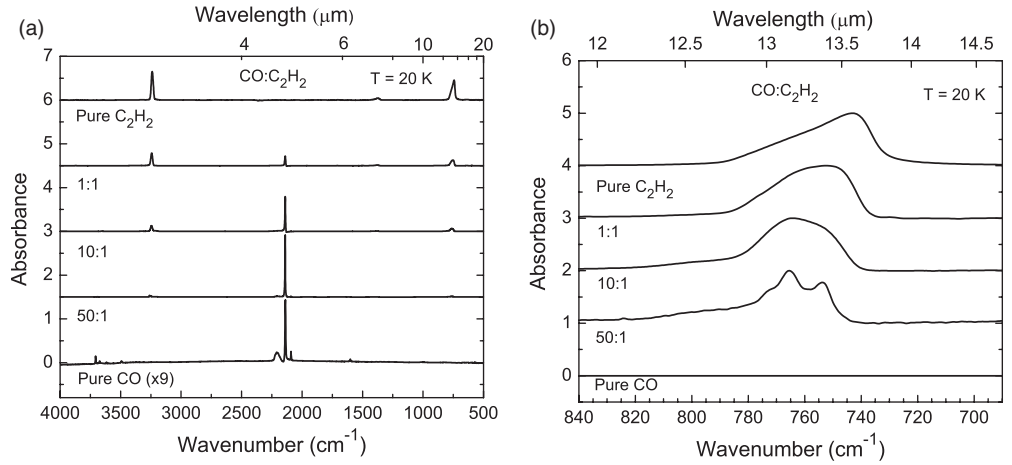

Figure 3. Infrared spectra of (a) $CO:C_2H_2$ mixtures with ratios 1:1, 10:1, and 50:1 compared to the spectra of pure CO and pure C_2H_2 and (b) enlargement of the ν_5 region. In (b) each spectrum is normalized to 1.

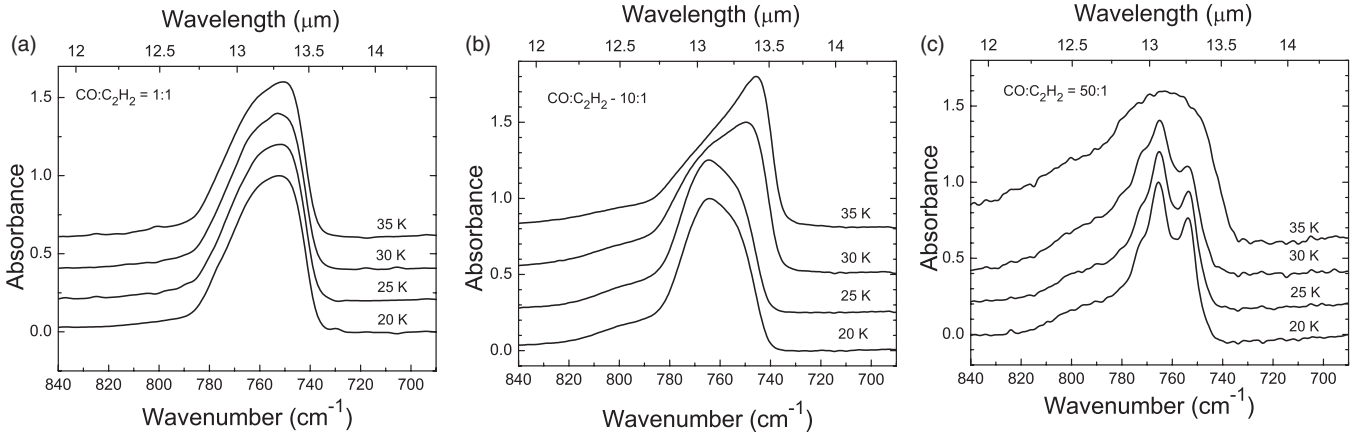

Figure 4. Infrared spectra of the ν_5 bending mode of C_2H_2 in $CO:C_2H_2$ mixtures with ratios of (a) 1:1, (b) 10:1, and (c) 50:1 as a function of temperature. All spectra were normalized to 1.

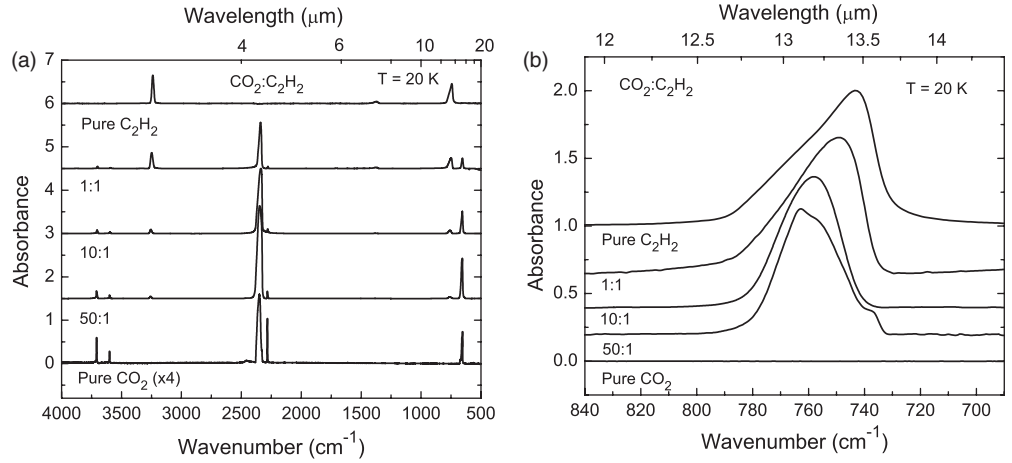

Figure 5. Infrared spectra of (a) $CO_2:C_2H_2$ mixtures with ratios 1:1, 10:1, and 50:1 compared to the spectra of pure CO_2 and pure C_2H_2 and (b) enlargement of the ν_5 region. In (b) each spectrum is normalized to 1.

ν_5 feature to develop a broader profile on its long-wavenumber side. For the $CO:C_2H_2$ (50:1) ice, the position of the ν_5-band maximum shifted about 20 cm^{-1} compared to the same band in pure C_2H_2, and was accompanied by splitting. Table 1 lists peak positions for the 50:1 ice. Since the ν_3 and ν_5 modes are split into two components, we list in Table 1 only the position of the strongest feature for each mode.

We calculated the intrinsic band strengths of C_2H_2 mixed with CO as a matrix gas (M) for a $CO:C_2H_2$ (50:1) sample using

$$A(\text{acetylene in M}) = \frac{N_{\text{M}}}{N_{\text{acetylene}}} \frac{\int \text{Abs}(\tilde{\nu})_{\text{acetylene in M}} d\tilde{\nu}}{\int \text{Abs}(\tilde{\nu})_{\text{M}} d\tilde{\nu}} A_{\text{M}}. \quad (2)$$

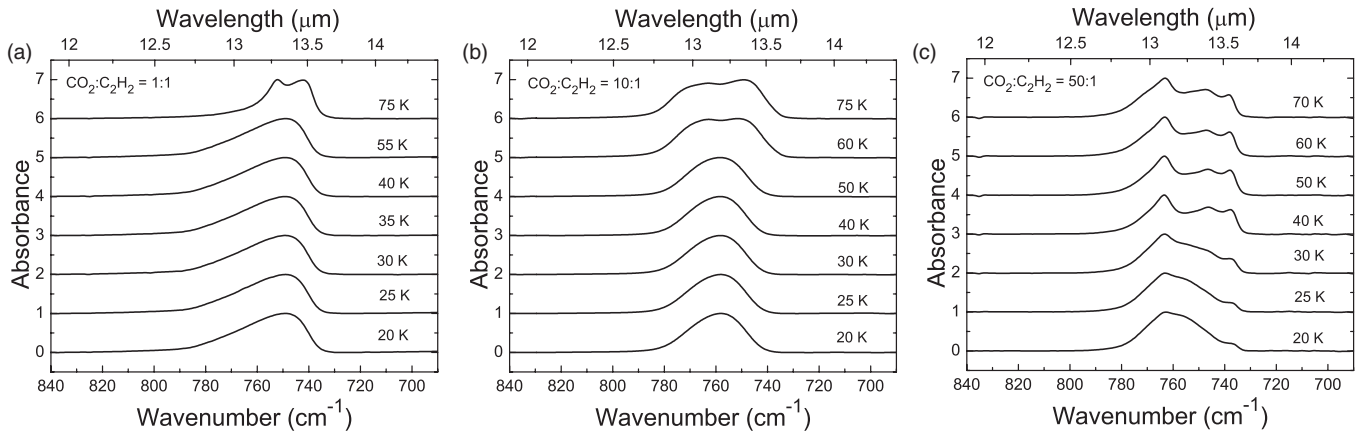

Figure 6. Infrared spectra of the ν_5 bending mode of C_2H_2 in CO_2:C_2H_2 mixtures with ratios of (a) 1:1, (b) 10:1, and (c) 50:1 as a function of temperature. All spectra were normalized to 1.

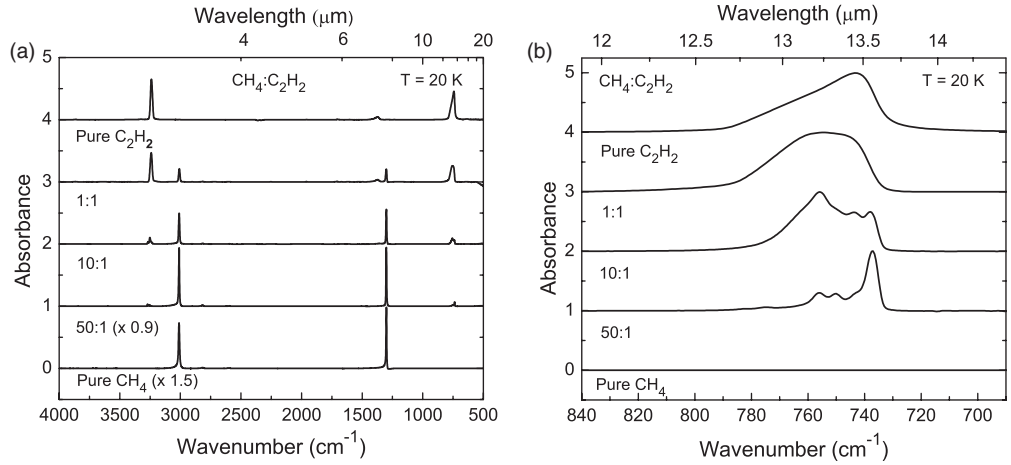

Figure 7. Infrared spectra of (a) CH_4:C_2H_2 mixtures with ratios 1:1, 10:1, and 50:1 compared to the spectra of pure CH_4 and pure C_2H_2 and (b) enlargement of the ν_5 region. In (b) each spectrum is normalized to 1.

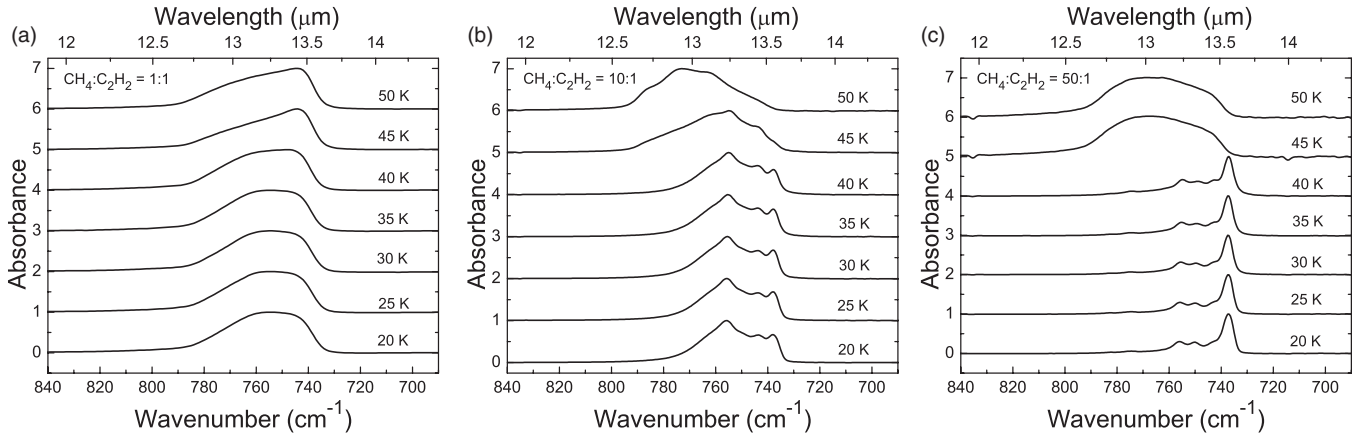

Figure 8. Infrared spectra of the ν_5 bending mode of C_2H_2 in CH_4:C_2H_2 mixtures with ratios of (a) 1:1, (b) 10:1, and (c) 50:1 as a function of temperature. All spectra were normalized to 1.

This same procedure was extended to C_2H_2-containing ices dominated by CO_2 (Section 3.1.3), CH_4 (Section 3.1.4), and H_2O (Section 3.1.5). The ratio of the column densities $N_M/N_{acetylene}$ was assumed to be the same as the ratio of gas pressures used during the mixing procedure. The following intrinsic band strengths were used: A(CO, 4252 cm^{-1}, 2.35 μm) = 1.6 × 10^{-19} cm molecule^{-1} (Gerakines et al. 2005), A(CO_2, 3708 cm^{-1}, 2.70 μm) = 1.4 × 10^{-18} cm molecule^{-1} (Gerakines et al. 1995), A(CH_4, 1301 cm^{-1}, 7.69 μm) = 3.8 × 10^{-18} cm molecule^{-1} (Hudgins et al. 1993), and A(H_2O, 3298 cm^{-1}, 3.03 μm) = 1.7 × 10^{-16} cm molecule^{-1} (Hudgins et al. 1993). Table 2 lists our A values for C_2H_2 in different matrices and compares our results with those of Boudin et al. (1998). The uncertainty in the A values calculated in Equation (2) for ice mixtures involves several terms. The ratio of column densities and the ratio of peak areas have uncertainties of ∼1% and

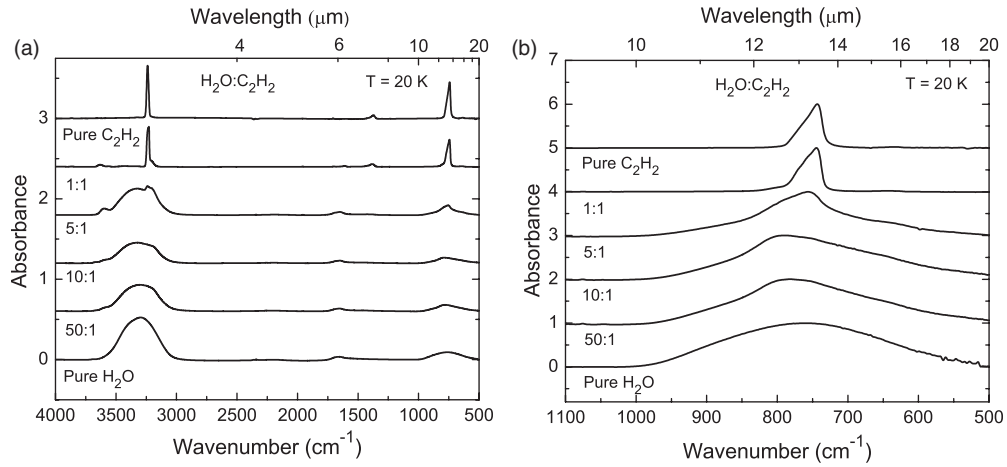

Figure 9. Infrared spectra of (a) H_2O:C_2H_2 mixtures with ratios 1:1, 5:1, 10:1, and 50:1 compared to the spectra of pure H_2O and pure C_2H_2 and (b) enlargement of the ν_5 region. In (b) each spectrum is normalized to 1.

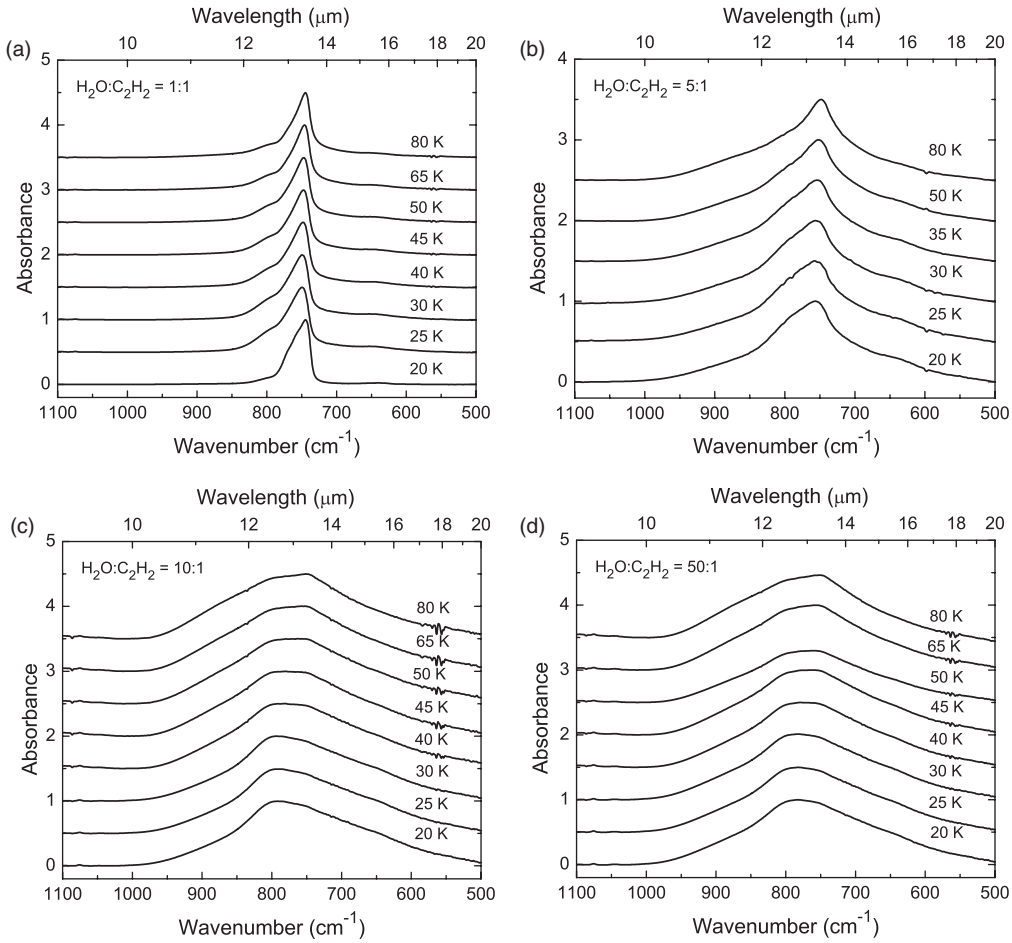

Figure 10. Infrared spectra of the ν_5 bending mode of C_2H_2 in H_2O:C_2H_2 mixtures with ratios of (a) 1:1, (b) 5:1, (c) 10:1, and (d) 50:1 as a function of temperature. All spectra were normalized to 1.

10%, respectively. Variations of 10% are reported for intensity values (used to determine A values) for CO and CO_2 matrices (Jiang et al. 1975; Yamada & Person 1964, respectively). A values for CH_4 and H_2O have uncertainties <30% (Hudgins et al. 1993).

Changes recorded in the 840–690 cm^{-1} (11.90–14.49 μm) region as three different CO:C_2H_2 ices were warmed are shown in Figure 4. The highest temperature presented for these mixtures is 35 K, since we knew that pure CO begins to sublime rapidly near 30 K in our vacuum system. For the 1:1 mixture, the band has a more rounded shape and a peak position 10 cm^{-1} higher than observed in pure C_2H_2. On warming to 35 K, the peak position fell by about 2 cm^{-1}. Spectra of the 10:1 mixture at 35 K showed an asymmetrical ν_5 band with a position very similar to that seen in the spectrum of pure C_2H_2, indicating that most of the volatile CO matrix ice had sublimed. When C_2H_2 was even more diluted (50:1), different associations of acetylene within the matrix appear to have been

present. This is supported by both low-level and high-level calculations which find that a C_2H_2 molecule can be hydrogen bonded with either the oxygen or carbon end of a CO molecule, and that these two arrangements are essentially isoenergetic (Parish et al 1992; Adamowicz 1992). However, only the linear structure where C_2H_2 is bonded with CO through the carbon end has been detected experimentally (Marshall et al. 1991). Self-aggregates of C_2H_2 may also be present in the 50:1 CO:C_2H_2 ice, contributing to the double-peaked spectrum.

3.1.3. CO_2:C_2H_2 Ice Mixtures

Figure 5(a) compares IR spectra of amorphous CO_2:C_2H_2 ices with spectra of C_2H_2 and CO_2. For these mixtures, increasing dilution caused the acetylene ν_5 band to develop a broader profile on its larger-wavenumber side, as shown in Figure 5(b) (a similar change was seen for ν_3). The peak also shifted to larger wavenumbers as the amount of CO_2 in the ice was increased. Table 1 lists C_2H_2 peak positions in the 50:1 CO_2:C_2H_2 sample. Although the ν_5 mode is split into two components, we list only the position of the strongest one in Table 1. Table 2 gives our A values for all three bands.

Changes in the 840–690 cm^{-1} (11.90–14.49 μm) region on warming are shown in Figure 6 for ices of three different CO_2:C_2H_2 ratios. The highest temperature presented for these mixtures is 75 K as we knew that rapid sublimation of pure CO_2 began near 85 K in our vacuum system. At 20 K, pure C_2H_2 and the 1:1 CO_2:C_2H_2 mixture show the same position for the acetylene ν_5 band and similar asymmetrical shapes. During warming, the peak position increases by about 7 cm^{-1}, and the band splits at 75 K. The C_2H_2 ν_5-band profile in the 10:1 mixture is more symmetrically shaped than that of pure C_2H_2, and the band position does not change on warming to 50 K; the band splits at 60 K. The larger bandwidth of the doublet at 75 K (compared to the doublet for the 1:1 mixture) suggests that C_2H_2 is interacting with either more or different sites within the CO_2 matrix. Similarly for the 50:1 mixture, the broad ν_5 band is present on deposit at 20 K and develops structure during warming to 70 K, which could be related to different associations of C_2H_2 within the ice. Possibilities are suggested by a calculation of Almeida (1990) showing that both parallel (side by side) and co-linear (end to end) associations are stable in solid CO_2. Self-aggregates of C_2H_2 also will be more isolated in a 50:1 CO_2:C_2H_2 mixture and will contribute to the spectrum.

3.1.4. CH_4:C_2H_2 Ice Mixtures

Figure 7(a) shows IR spectra of amorphous CH_4:C_2H_2 ices compared with spectra of C_2H_2 and CH_4. For these ices, the ν_5 C_2H_2 band changes with dilution as shown in Figure 7(b). The region around the maximum of the ν_5 band of the 1:1 CH_4:C_2H_2 mixture is flatter than for the corresponding acetylene absorbance in pure C_2H_2. With dilution, at least four peaks within the band are observed, suggesting different aggregate sites. Table 1 lists C_2H_2 peak positions in the 50:1 CH_4:C_2H_2 ice. Although the ν_3, ν_4 + ν_5, and ν_5 modes are split into four components, Table 1 lists only the position of the strongest feature in each mode. Table 2 gives A values for each multiplet.

Figure 8 shows how warming caused changes in the 840–690 cm^{-1} (11.90–14.49 μm) region for CH_4:C_2H_2 ices. The highest temperature presented for these mixtures is 50 K as we knew that pure CH_4 sublimed rapidly near 40 K in our vacuum system. For the 1:1 mixture, the ν_5 band is a rounded feature with a flat top that does not change from 20 to 40 K. At 45–50 K, the asymmetrical feature that forms is similar to that seen for C_2H_2 at 40–45 K (Figure 2(b)), perhaps due to C_2H_2 crystallization in each case. Even at 50 K the ice had not fully crystallized perhaps because it had trapped some CH_4. For the 10:1 mixture at 45 K, the spectrum shows small features that probably represent interacting species. At 50 K we expect that most of the CH_4 has sublimed. The structure (splitting and shift) of the spectral feature resembles what is seen as ices crystallize, although the center of the entire C_2H_2 band is ~12 cm^{-1} higher in wavenumbers than seen in the spectrum of pure C_2H_2 held at 50 K. This variation again could be due to residual CH_4 trapped within the ice. The profiles of the acetylene ν_5 band for the 10:1 and 50:1 mixtures show (Figure 8) that at least four sites are present when the ice was made at 20 K. The sites are stable during warming from 20 to 40 K, although their relative occupancies differ for the two ice concentrations. It is interesting to note that the most intense peak position for 50:1 CH_4:C_2H_2 at 20 K is smaller by ~5 cm^{-1} than the position observed in C_2H_2 itself. In the 50:1 ice, the entire CH_4 matrix sample has sublimed at 45 K. Studies of matrix-isolated C_2H_2, where the matrix:C_2H_2 ratio is on the order of 2000, show evidence for the isolation of C_2H_2 monomers, dimers, and polymers (Bagdanskis & Bulanin 1972). In recent computational work (Bango et al. 2003), the existence of intermolecular bonding between C_2H_2 and CH_4 was investigated. The structure is optimized when a hydrogen from CH_4 is near the carbon–carbon triple bond electron cloud of acetylene essentially at a 90° angle. In the same study, it was shown that the C_2H_2–C_2H_2 interaction is almost four times stronger than the CH_4–C_2H_2 interaction. Therefore, we expect that the spectrum of 50:1 CH_4:C_2H_2 is some combination of self-associated C_2H_2 molecules along with complexes that form between methane and acetylene, with C_2H_2 self-association preferred.

3.1.5. H_2O:C_2H_2 Ice Mixtures

Figure 9 shows IR spectra of amorphous H_2O, C_2H_2, and H_2O:C_2H_2 ices. The last is the only ice mixture we studied in which both the ν_3 and ν_5 absorption bands of C_2H_2 overlapped with absorptions of the matrix ice (the OH stretch and the libration band of H_2O, respectively). Therefore, it was often difficult if not impossible to separate the C_2H_2 and H_2O bands. Figure 9(b) shows that with increasing H_2O the C_2H_2 band becomes more difficult to see. Therefore, for these ices Table 1 gives the peak position of only the acetylene ν_4 + ν_5 and ν_5 features, and Table 2 lists the A value for only the combination band. Tables 1 and 2 refer to H_2O:C_2H_2 (5:1) ices.

Changes in the 1100–500 cm^{-1} (9.09–20 μm) region as the ice is warmed can be seen in Figure 10. Even at 80 K, the highest temperature presented, C_2H_2 does not crystallize since it is trapped and diluted within the H_2O matrix. For the 1:1 mixture, the acetylene ν_5 band has an asymmetrical shape with a peak position 2 cm^{-1} above that seen for C_2H_2. The band is unchanged with warming. The C_2H_2 ν_5 peak position in the 5:1 mixture is shifted 13 cm^{-1} to larger wavenumbers compared to that of C_2H_2 at 20 K. The band profile broadens significantly on warming. Silva & Devlin (1994) examined the interaction of C_2H_2 with H_2O-ice surfaces by studying the 3300 cm^{-1} (3 μm) region of the IR spectrum. Their experiments and calculations supported the idea that C_2H_2 interacts as either a proton donor (an end-on structure, H–CC–H ••• OH_2) or as a proton acceptor (a perpendicular structure, HO–H ••• center of H–CC–H). They were able to resolve and assign such features to components of the ν_3 mode of C_2H_2 near

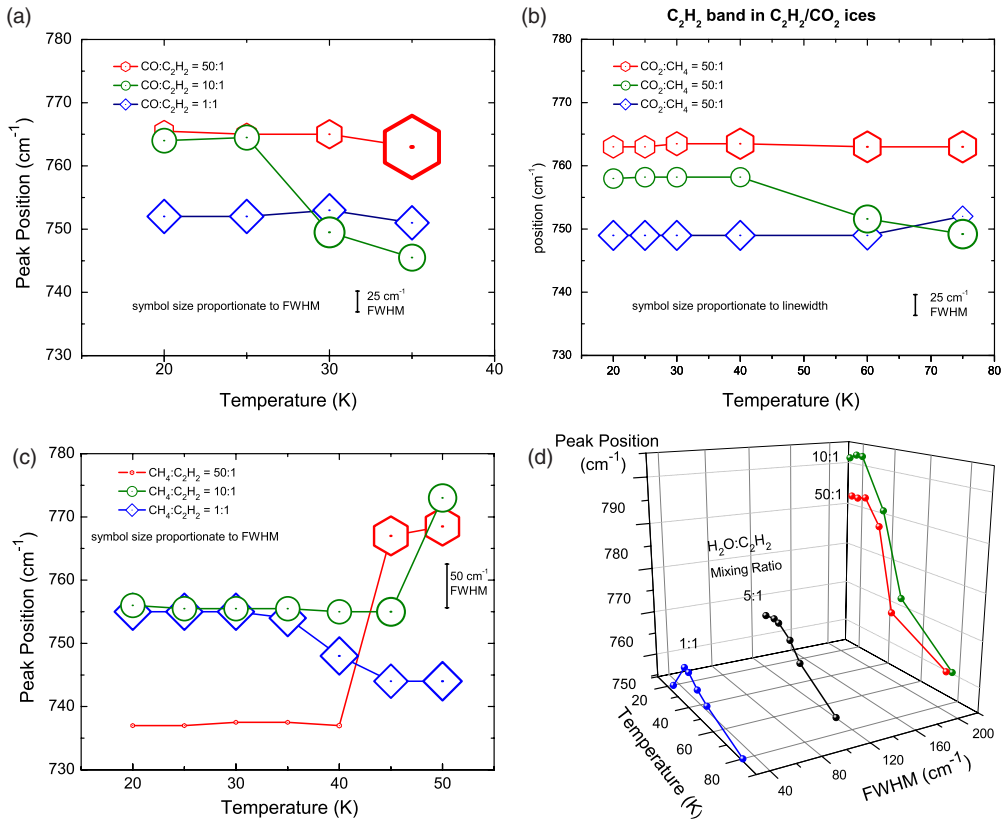

Figure 11. Variation of the FWHM of the ν_5 bending mode of solid C_2H_2 in (a) $CO:C_2H_2$, (b) $CO_2:C_2H_2$, (c) $CH_4:C_2H_2$, and (d) $H_2O:C_2H_2$ mixtures as a function of mixing ratio at different temperatures. For (a), (b), and (c), the symbol size is scaled to represent the FWHM, whereas the center of each symbol is the peak position. Compare the length of the scale bar in (a), (b), and (c) with the size of the symbol to get an indication of the FWHM value. (d) is a three-dimensional plot for the $H_2O:C_2H_2$ mixtures. Table 3 tabulates most FWHM values.

(A color version of this figure is available in the online journal.)

3200 cm^{-1}. The broadening we observed may correspond to unresolved features of these different bonding arrangements. Ab initio computations by Rovira et al. (1995) showed that these two arrangements are about equally bound. However, Silva & Devlin (1994) pointed out that the picture is more complex as the temperature changes since the perpendicular complex was preferred at 50 K. Unfortunately, IR features of these associations are not seen in either our 10:1 or 50:1 mixtures since the C_2H_2 absorbance is indistinguishable from the broad libration band of H_2O, although the general shift of the peak maxima to lower wavenumbers as the temperature increases may be an indicator of that effect.

3.2. Bandwidth

The FWHM of the ν_5 C_2H_2 band is plotted as a function of temperature for different mixtures in Figure 11. Table 3 summarizes these data. The line width for C_2H_2 in CO, CO_2, and CH_4 varies significantly with temperature and concentration while the line width in H_2O depends on concentration alone. The measured width of the C_2H_2 feature is near 30 cm^{-1} at 20 K for pure C_2H_2. It is interesting to note that at 20 K the width of this band decreases to 25, 26, and 6 cm^{-1} when diluted in CO, CO_2, and CH_4, respectively, with a matrix: C_2H_2 ratio of 50:1. The width of the C_2H_2 feature similarly diluted in H_2O is roughly 200 cm^{-1}. Such a large FWHM value occurs because the ν_5 band of C_2H_2 overlaps with the broad libration band of H_2O which dominates the spectrum. Meaningful differences between H_2O and $H_2O:C_2H_2$ (50:1) spectra cannot be determined. However, even in the 5:1 mixture the C_2H_2 feature has an FWHM bandwidth of 120 cm^{-1}. This shows a well-known trend of increasing width in a polar matrix, which has been documented for the CO fundamental (Sandford et al. 1988). For the more volatile matrices, CO and CH_4, the sudden increase in the bandwidth for the 50:1 mixtures, and the loss of peak structure, corresponds to the vaporization of the matrix.

4. ASTROPHYSICAL IMPLICATIONS

We have measured IR spectra from 4000 to 500 cm^{-1} (2.5–20 μm) of C_2H_2 and of C_2H_2-containing ices dominated by CO, CO_2, CH_4, and H_2O. Both temperature and concentration (for the mixtures) have been varied systematically. We have included additional spectral details here about the acetylene ν_5 band (743 cm^{-1}, 13.46 μm) as it is the strongest C_2H_2 feature within the 5–20 μm observing range of *Spitzer*/IRS. The value of our database of ice spectra is that it covers a broad range of temperature and composition and was acquired with a consistent procedure in a single laboratory.

Although many reports of interstellar ices dominated by amorphous H_2O have been published, the results described here show that astronomical detections of C_2H_2 in such ices will be difficult. The broad libration feature of the H_2O-ice IR spectrum is superimposed on the acetylene ν_5 band making it difficult to see small amounts of C_2H_2 in H_2O-rich solids, as noted earlier. It is only possible to confidently deconvolve these two bands when C_2H_2 is about 20% or more of the mixture. Similar comments

Table 3
Peak Position (cm^{-1}) and FWHM (cm^{-1}) for ν_5 C_2H_2

Mixture	Mixing	20 K		30 K		40 K		50 K		80 K	
	Ratio	$\tilde{\nu}$	FWHM	$\tilde{\nu}$	FWHM	$\tilde{\nu}$	FWHM	$\tilde{\nu}$	FWHM	$\tilde{\nu}$	FWHM
C_2H_2		743	30	743	31	744	33	758	39	760	35
$CO:C_2H_2$	1:1	752	34	752	34	...	...	...	...	...	...
$CO:C_2H_2$	10:1	764	31	750	38	...	...	...	...	...	...
$CO:C_2H_2$	50:1	766	25	765	33	...	...	...	...	...	...
$CO_2:C_2H_2$	1:1	749	30	749	30	749	30			*752	*21
$CO_2:C_2H_2$	10:1	758	25	758	25	758	24	...	...	*749	*37
$CO_2:C_2H_2$	50:1	763	26	764	28	764	36	...	...	*763	*37
$CH_4:C_2H_2$	1:1	755	37	755	37	748	38	744	39	...	...
$CH_4:C_2H_2$	10:1	756	30	756	30	755	30	773	35	...	...
$CH_4:C_2H_2$	50:1	737	6	738	5	737	6	768	44	...	...
$H_2O:C_2H_2$	1:1	744	35	750	40	748	38	747	36	744	32
$H_2O:C_2H_2$	5:1	757	122	757	122	755	120	752	116	748	106
$H_2O:C_2H_2$	10:1	792	206	793	204	782	210	762	214	752	212
$H_2O:C_2H_2$	50:1	783	209	784	208	778	206	760	204	752	206

Note. * Temperature was 75 K for these ices.

apply for the acetylene ν_3 band (~3200 cm^{-1}, ~3.125 μm), which is obscured by stretching vibrations of H_2O-ice. For more dilute mixtures, subtraction of the H_2O band from the spectrum of an $H_2O:C_2H_2$ mixture produces a weak residual with little resemblance in position, line width, or band shape to the pure C_2H_2 feature.

Our laboratory results show that acetylene is better distinguished in non-polar and weakly polar ices such as CO, CO_2, and CH_4. In each of these matrices, the acetylene ν_5 feature shows unique multiple peaks for a 50:1 ice mixture, probably due to various complexes formed between C_2H_2 and the matrix molecules. While CO and CH_4 ices tend to rapidly sublime under vacuum at 30–35 K, CO_2-ice persists to about 90 K and is most likely to show IR evidence of traces (e.g., 2%) of C_2H_2 over a reasonably wide temperature range (e.g., 20–70 K).

The present work demonstrates that a large range of peak positions, peak widths, and complex band shapes exist for the acetylene ν_5 feature, and shows that these depend on ice composition and temperature. For example, Table 1 gives the peak of the C_2H_2 ν_5 band in a 50:1 $CO:C_2H_2$ mixture as 765 cm^{-1} at 20 K, but 763 and 737 cm^{-1} in CO_2 and CH_4 matrices, respectively. Such variations emphasize the need for a systematic, uniform set of C_2H_2 spectra recorded under a variety of conditions to aid in detection of acetylene with infrared-astronomical observations.

Figure 12 compares selected laboratory ice data with the 750 cm^{-1} region observed along the Serpens-source line of sight in the Serpens dark cloud with $A_v \sim 25$ mag. The observation was part of the c2d Legacy program (Evans et al. 2003). It was obtained with the short-wavelength, low-resolution module (SL; $\lambda = 5$–$14\,\mu$m, $R \equiv \lambda/\Delta\lambda = 64$–$128$), with on-source integration times of 28 s per spectral order. The S16 data from the Spitzer Science Center Archive were used. Customized source extractions were performed with routines similar to those of Boogert et al. (2011). Because the acetylene ν_5 band lies in a region affected by the silicate absorption feature and the libration band of H_2O-ice, it was difficult to extract a residual with a low signal-to-noise ratio in the 750 cm^{-1} region, as previously noted. Therefore, we compare our laboratory data with the original optical depth spectrum.

The Serpens-source spectrum from 1800 to 500 cm^{-1} is shown expanded in the 750 cm^{-1} region where it is compared with 20 K spectra of pure C_2H_2 and the C_2H_2 band in the most

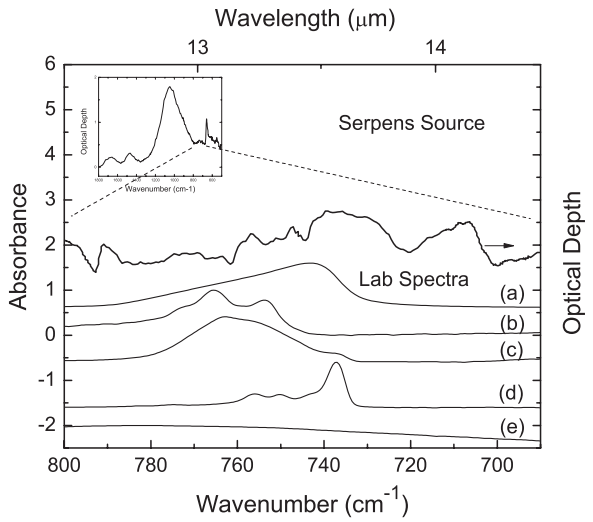

Figure 12. Spectrum of Serpens source (2MASS 18285266 + 0028242) is shown in the inset and expanded in the 800–690 cm^{-1} range. Laboratory spectra of 20 K C_2H_2 ices are compared with this observational data. Spectra are (a) pure C_2H_2, and 50:1 mixtures of (b) $CO:C_2H_2$, (c) $CO_2:C_2H_2$, (d) $CH_4:C_2H_2$, and (e) $H_2O:C_2H_2$. The arrow indicates that the observed spectrum is on an optical depth scale, whereas lab spectra are on an absorbance scale.

dilute matrices. It is clear that none of the laboratory spectra in Figure 12 are a good match with the observations. We also attempted to combine various spectra at different temperatures to approximately fit the observations. The only spectra showing similar features were those containing 50:1 $CH_4:C_2H_2$ ice at 40 K. Originally, the CH_4 abundance in the sight line for the Serpens source was reported to be ~3% relative to H_2O (Knez et al. 2008) although its presence is hard to detect in the spectrum in the 1300 cm^{-1} region in Figure 12. Therefore, further searches for C_2H_2 in dark quiescent clouds such as the Serpens source await new observational data with sufficiently high signal-to-noise ratio.

Acetylene remains a very strong candidate for further searches. The spectra of ices we have measured can be used to fit observations to help provide important information about the solid-state inventory and temperature of ices in dense cloud regions. All of our spectra are currently available in digital format at http://science.gsfc.nasa.gov/691/cosmicice.

The authors acknowledge support through NASA's Outer Planets, Cassini Data Analysis, and Planetary Atmospheres programs, and The Goddard Center for Astrobiology. The authors thank S. Travis for help with some of the experiments, P. Gerakines for assistance with graphics, A. Boogert for providing tools for reducing the *Spitzer* spectrum, and Z. Peeters for useful discussions.

REFERENCES

Adamowicz, L. 1992, Chem. Phys. Lett., 192, 199
Almeida, W. B. 1990, Chem. Phys., 141, 297
Bagdanskis, N. I., & Bulanin, M. O. 1972, Opt. Spectrosc., 32, 525
Bango, A., Casella, G., Saielli, G., & Scorrano, G. 2003, Int. J. Mol. Sci., 4, 193
Boogert, A. C. A., Huard, T. L., Cook, A. M., et al. 2011, ApJ, 729, 92
Bottger, G. L., & Eggers, D. F., Jr 1964, J. Chem. Phys., 40, 2010
Boudin, N., Schutte, W. A., & Greenberg, J. M. 1998, A&A, 331, 749
Brown, R. H., Cruikshank, D. P., Tokunaga, A. T., Smith, R. G., & Clark, R. N. 1988, Icarus, 74, 262
Chiar, J. E., Adamson, A. J., Kerr, T. H., & Whittet, D. C. B. 1994, ApJ, 426, 240
Chiar, J. E., Adamson, A. J., Kerr, T. H., & Whittet, D. C. B. 1995, ApJ, 455, 234
Chiar, J. E., Pendleton, Y. J., Allamandola, L. J., et al. 2011, ApJ, 731, 9
Dows, D. 1966, Spectrochim. Acta, 22, 1479
Evans, N. J., II, Allen, L. E., Blake, G. A., et al. 2003, PASP, 115, 965
Evans, N. J., Lacy, J. H., & Carr, J. S. 1991, ApJ, 383, 674
George, L., Sanchez-Garcia, E., & Sander, W. 2003, J. Phys. Chem. A, 107, 6850
Gerakines, P. A., Bray, J. J., Davis, A., & Richey, C. R. 2005, ApJ, 620, 1140
Gerakines, P. A., Schutte, W. A., Greenberg, J. M., & van Dishoeck, E. F. 1995, A&A, 296, 810
Gibb, E. L., Whittet, D. C. B., Boogert, A. C. A., & Tielens, G. G. M. 2004, ApJS, 151, 35
Gough, T. E., & Rowat, T. E. 1998, J. Chem. Phys., 109, 6809
Hudgins, D. M., Sandford, S. A., Allamandola, L. J., & Tielens, A. G. G. M. 1993, ApJS, 86, 713
Hudson, R. L., & Moore, M. H. 2004, Icarus, 172, 466
Jiang, G. J., Person, W. B., & Brown, K. G. 1975, J. Chem. Phys., 82, 1201
Khanna, R. K., Ospina, M. J., & Zhao, G. 1988, Icarus, 73, 527
Knez, C., Boogert, A. C. A., Pontoppidan, K. M., et al. 2005, ApJ, 635, L145
Knez, C., Moore, M., Travis, S., et al. 2008, in IAU Symp. 251, Organic Matter in Space, ed. S. Kwok & S. Sandford (Cambridge: Cambridge Univ. Press), 47
Lacy, J. H., Evans, N. J., Achtermann, J. M., et al. 1989, ApJ, 342, L43
Lahuis, F., & van Dishoeck, E. F. 2000, A&A, 355, 699
Lee, Y.-C., Venkatesan, V., Lee, Y.-P., et al. 2007, Chem. Phys. Lett., 435, 247
Marshall, M. D., Kim, J., Hu, T. A., Sun, L. H., & Muenter, J. S. 1991, J. Chem. Phys., 94, 6334
Moore, M. H., & Hudson, R. L. 2003, Icarus, 161, 486
Mumma, M. J., & Charnley, S. B. 2011, ARA&A, 49, 471
Mumma, M. J., Disanti, M. A., dello Russo, N., et al. 2003, Adv. Space Res., 31, 2563
Nguyen, T. K., Viti, S., & Williams, D. A. 2002, A&A, 387, 1083
Öberg, K. I., Boogert, A. D. A., Pontoppidan, K. M., et al. 2011, ApJ, 740, 109
Öberg, K. I., Boogert, A. D. A., Pontoppidan, K. M., et al. 2008, ApJ, 678, 1032
Parish, C. A., Augspurger, J. D., & Dykstra, J. 1992, J. Phys. Chem., 96, 2069
Rovira, M. C., Novoa, J. J., Whangbo, M.-H., & Williams, J. M. 1995, Chem. Phys., 200, 319
Sandford, S. A., Allamandola, J. J., Tielens, A. G. G. M., & Valero, G. J. 1988, ApJ, 329, 498
Silva, S. C., & Devlin, J. P. 1994, J. Phys. Chem., 98, 10847
Stäuber, P., Doty, S. D., van Dishoeck, E. F., & Benz, A. O. 2005, A&A, 440, 949
Stäuber, P., Doty, S. D., van Dishoeck, E. F., Jørgensen, J. K., & Benz, A. O. 2004, A&A, 425, 577
Whittet, D. C. B., Gerakines, P. A., Tielens, A. G. G. M., et al. 1998, ApJ, 498, L159
Whittet, D. C. B., Schutte, W. A., Tielens, A. G. G. M., et al. 1996, A&A, 315, L357
Yamada, H., & Person, W. B. 1964, J. Chem. Phys., 41, 2478